

Quantum spin Hall effect induced by electric field in silicene

Xing-Tao An,^{1,2} Yan-Yang Zhang,^{2,3, a)} Jian-Jun Liu,⁴ and Shu-Shen Li²

¹⁾*School of Sciences, Hebei University of Science and Technology, Shijiazhuang, Hebei 050018, China*

²⁾*SKLSM, Institute of Semiconductors, Chinese Academy of Sciences, P. O. Box 912, Beijing 100083, China*

³⁾*International Center for Quantum Materials, Peking University, Beijing 100871, China*

⁴⁾*Physics Department, Shijiazhuang University, Shijiazhuang 050035, China*

(Dated: 28 March 2022)

We investigate the transport properties in a zigzag silicene nanoribbon in the presence of an external electric field. The staggered sublattice potential and two kinds of Rashba spin-orbit couplings can be induced by the external electric field due to the buckled structure of the silicene. A bulk gap is opened by the staggered potential and gapless edge states appear in the gap by tuning the two kinds of Rashba spin-orbit couplings properly. Furthermore, the gapless edge states are spin-filtered and are insensitive to the non-magnetic disorder. These results prove that the quantum spin Hall effect can be induced by an external electric field in silicene, which may have certain practical significance in applications for future spintronics device.

PACS numbers: 73.20.At, 73.22.-f, 73.63.-b

Keywords: Silicene; Quantum spin Hall effect

Recently, the quantum spin Hall effect (QSHE) has attracted significant interests in the fields of condensed matter physics and material science as it constitutes a new phase of matter and has potential applications in spintronics.¹⁻⁵ The novel electronic state with a nontrivial topological property and time-reversal invariance has a bulk energy gap separating the valence and conduction bands and a pair of gapless spin-filtered edge states at the sample boundaries. The QSHE has been first predicted by Kane and Mele in graphene in which the intrinsic spin-orbit coupling opens a band gap at the Dirac points.¹ However, the QSHE can occur in graphene only at unrealistically low temperatures since the intrinsic spin-orbit coupling in graphene is rather weak.⁶⁻⁸ Therefore, it is crucial to search new materials with strong spin-orbit coupling for realizing the QSHE. Recent theories and experiments provide evidences of the QSHE in two-dimensional HgTe-CdTe quantum wells.^{2,3}

Very recently, a close relative of graphene, a slightly buckled honeycomb lattice of Si atoms called silicene has been synthesized.⁹⁻¹³ Silicene can be well compatible with current silicon based electronic technology. Many progresses in the study of silicene have been made, both experimentally and theoretically. For example, electronic properties and the giant magnetoresistance in silicene have been reported.¹⁴⁻¹⁷ Moreover, almost every striking property of graphene could be transferred to silicene.^{13,18} It has been theoretically shown that the strong intrinsic spin-orbit coupling in silicene may lead to detectable QSHE.^{5,19-23}

In this paper, we provide systematic investigations on the band structures and electron transport properties of

silicene in the presence of an external electric field. Silicene consists of a buckled honeycomb lattice of silicon atoms with two sublattices A and B. We take a silicene sheet on the $x - y$ plane, and apply the electric field in z direction. The electric field generates a staggered sublattice potential between silicon atoms at A sites and B sites due to the buckled structure of the silicene. On the other hand, two kinds of Rashba spin-orbit coupling, referring to the nearest and next-nearest neighbor hoppings respectively, can also be tuned by the external electric field. We find that a gap can be opened by the staggered sublattice potential and gapless edge states are induced in the gap by Rashba spin-orbit coupling. We predict that the QSHE can be observed by applying an external electric field in silicene even if the intrinsic spin-orbit coupling in the system is very weak.

In the tight-binding representation, the silicene sample with an external electric field can be described by the the following Hamiltonian:²⁰

$$\begin{aligned}
 H = & -t \sum_{\langle ij \rangle \alpha} c_{i\alpha}^\dagger c_{j\alpha} + \sum_{i\alpha} \varepsilon_i \mu_{ij} c_{i\alpha}^\dagger c_{i\alpha} \\
 & + i\lambda_{R1} \sum_{\langle ij \rangle \alpha\beta} c_{i\alpha}^\dagger (\vec{\sigma} \times \vec{d}_{ij}^0)_{\alpha\beta}^z c_{j\beta} \\
 & - i\frac{2}{3}\lambda_{R2} \sum_{\langle\langle ij \rangle\rangle \alpha\beta} \mu_{ij} c_{i\alpha}^\dagger (\vec{\sigma} \times \vec{d}_{ij}^0)_{\alpha\beta}^z c_{j\beta}, \quad (1)
 \end{aligned}$$

where $c_{i\alpha}^\dagger$ creates an electron with spin polarization α at site i ; $\langle ij \rangle$ and $\langle\langle ij \rangle\rangle$ run over all the nearest and next-nearest neighbor hopping sites, respectively. The first term is the nearest-neighbor hopping with the transfer energy $t = 1.6eV$. The second term is the staggered sublattice potential term, where $\mu_{ij} = \pm 1$ for the A (B) site and ε_i is the potential energy induced by the external electric field. The third and fourth terms, re-

^{a)}Electronic mail: yanyang@semi.ac.cn

spectively, represent the first Rashba spin-orbit coupling associated with the nearest neighbor hopping and the second Rashba spin-orbit coupling associated with the next-nearest neighbor hopping. Both of them are induced by the external electric field. Here $\vec{\sigma} = (\sigma_x, \sigma_y, \sigma_z)$ is the Pauli matrix of spin and $\vec{d}_{ij}^0 = \vec{d}_{ij}/|\vec{d}_{ij}|$ with the vector \vec{d}_{ij} connecting two sites i and j . The intrinsic SOC term has been ignored intentionally since the main focus of this work is the Rashba terms and the staggered potential, which can be tuned by the external electric field.

We assume that the temperature is set to zero and two semi-infinite silicene ribbons are employed as left and right leads. The two-terminal conductance of the system can be calculated by the nonequilibrium Green's function method and Landauer-Büttiker formula as

$$G(E) = \frac{e^2}{h} \text{Tr}[\Gamma_L(E)\mathbf{G}^r(E)\Gamma_R(E)\mathbf{G}^a(E)], \quad (2)$$

where $\Gamma_p(E) = i[\Sigma_p^r(E) - \Sigma_p^a(E)]$ is the line-width function and $\mathbf{G}^r(E) = [\mathbf{G}^a(E)]^\dagger = 1/[\mathbf{E} - \mathbf{H}_{cen} - \Sigma_L^r - \Sigma_R^r]$ is the retarded Green function with the Hamiltonian in the center region \mathbf{H}_{cen} .²⁴ The self-energy Σ_p^r due to the semi-infinite lead- p can be calculated numerically.²⁵

With the help of the nonequilibrium Green's function method, the local current flowing on site i with spin σ can be expressed as

$$J_{i\sigma} = \sum_{j\sigma'} J_{i\sigma,j\sigma'} = -\frac{e}{\hbar} \sum_{j\sigma'} [H_{i\sigma,j\sigma'} G_{j\sigma',i\sigma}^<(t,t) - G_{i\sigma,j\sigma'}^<(t,t) H_{j\sigma',i\sigma}], \quad (3)$$

where $G_{i\sigma,j\sigma'}^< = i\langle c_{j\sigma'}^\dagger c_{i\sigma} \rangle$ is the matrix element of the lesser Green's function of the scattering region and $J_{i\sigma,j\sigma'}$ is the current from site i to j . After taking Fourier transformation, the local current $J_{i\sigma,j\sigma'}$ can be calculated as

$$J_{i\sigma,j\sigma'} = -\frac{2e}{\hbar} \int \frac{dE}{2\pi} \text{Re}[H_{i\sigma,j\sigma'} G_{j\sigma',i\sigma}^<(E)]. \quad (4)$$

Eq. (4) has been widely used in the local-current studies of tight-binding models.²⁶⁻²⁸ When the sample is at zero temperature and the applied voltage is small, by applying the Keldysh equation $G^< = G^r(i\Gamma_L f_L + i\Gamma_R f_R)G^a$ with the Fermi distribution function $f_p = f_0(E + eV_p)$,²⁹ the Eq. (4) can be written as

$$J_{i\sigma,j\sigma'} = \frac{2e}{\hbar} \int_{-\infty}^{eV_R} dE \text{Im}\{H_{i\sigma,j\sigma'} [G^r(\Gamma_L + \Gamma_R)G^a]_{j\sigma',i\sigma}\} + \frac{2e^2}{\hbar} (V_L - V_R) \text{Im}[H_{i\sigma,j\sigma'} G_{j\sigma',i\sigma}^n(E)], \quad (5)$$

where V_L and V_R are the voltages at the Lead-L and R, respectively. $G^n(E) = G^r(E)\Gamma_L(E)G^a(E)$ is electron correlation function. The first part of Eq. (5) can only generate the equilibrium current and does not contribute to the transport, so it can be dropped out in present work. It is the second part that gives rise to the nonequilibrium current.

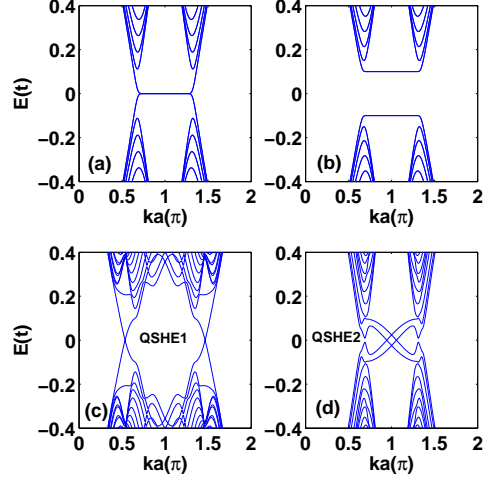


FIG. 1. Calculated energy bands in the zigzag nanoribbon geometry for (a) $\varepsilon_i = 0$, $\lambda_{R1} = 0$ and $\lambda_{R2} = 0$, (b) $\varepsilon_i = 0.1t$, $\lambda_{R1} = 0$ and $\lambda_{R2} = 0$, (c) $\varepsilon_i = 0.1t$, $\lambda_{R1} = 1.0t$ and $\lambda_{R2} = 0.2t$, and (d) $\varepsilon_i = 0.1t$, $\lambda_{R1} = 0.05t$ and $\lambda_{R2} = 0.6t$.

In the following numerical calculations, we use the hopping energy t as the energy unit. The width of the zigzag ribbon is $59a$, where a is the silicon-silicon distance. In Fig. 1 we show the energy bands obtained from diagonalizing the tight-binding Hamiltonian (1) with various parameters for a zigzag nanoribbon. The nanoribbon with only the nearest-neighbor hopping shows a semi-metallic behavior, as shown in Fig. 1 (a). An energy gap can be opened due to the inversion symmetry breaking induced by the staggered sublattice potential and the magnitude of the gap is $2\varepsilon_i$ (see Fig. 1 (b)). When the first and second Rashba spin-orbit couplings induced by the external electric field are taken into account properly, which turn silicene from normal insulating to quantum spin Hall regime, gapless edge states appear within the band gap (see Figs. 1 (c) and (d)). The gapless edge states with different spins connect the conduction band and valence band. As usual, these gapless edge states are originated from the nontrivial topological orders in the bulk. According to different values of the first Rashba spin-orbit coupling, the QSHE induced by the external electric field can be divided into two types, QSHE1 and QSHE2. In QSHE1, when the first Rashba spin-orbit coupling is strong, the edge states traverse the bulk gap *within* each valley, as shown in Fig. 1 (c). However, in QSHE2 when the first Rashba spin-orbit coupling is weak, the edge states inter-connect two valleys. Moreover, they bend and give rise to “subgaps” around K and K' , which makes the structure of propagating channels complicated in the bulk gap.

To investigate the QSHE induced by the external electric field in more details, the configurations of the spin-dependent local-current-flow vector are plotted in Fig. 2. We focus only on the left-injected current. The Fermi

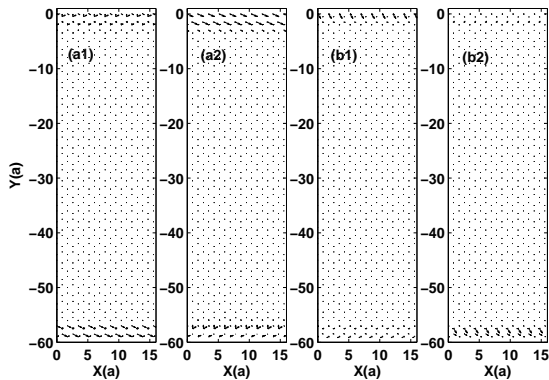


FIG. 2. The local spin-up (a1 and b1) and spin-down (a2 and b2) currents density vector distribution for (a) $\varepsilon_i = 0.1t$, $\lambda_{R1} = 1.0t$ and $\lambda_{R2} = 0.2t$ (QSHE1) with $E = 0.05t$, and for (b) $\varepsilon_i = 0.1t$, $\lambda_{R1} = 0.05t$ and $\lambda_{R2} = 0.6t$ (QSHE2) with $E = 0.005t$.

energy is set to be $E = 0.05t$ for QSHE1 (Fig. 2 (a)) and $E = 0.005t$ for QSHE2 (Fig. 2 (b)). For these Fermi energies, there are only the lowest transmission channels, i.e., the gapless edge states. For QSHE1, the spin-up local currents locate mainly on the lower edge (see Fig. 2 (a1)) and the spin-down local currents locate mainly on the upper edge (see Fig. 2 (a2)). Contrary to QSHE1, for QSHE2, the spin-up local currents locate mainly on the upper edge (see Fig. 2 (b1)) and the spin-down local currents locate mainly on the lower edge (see Fig. 2 (b2)). These results show that the gapless edge states are spin-filtered and the two kinds of Rashba spin-orbit couplings can drive an ordinary insulating state of the silicene to the topological insulator.

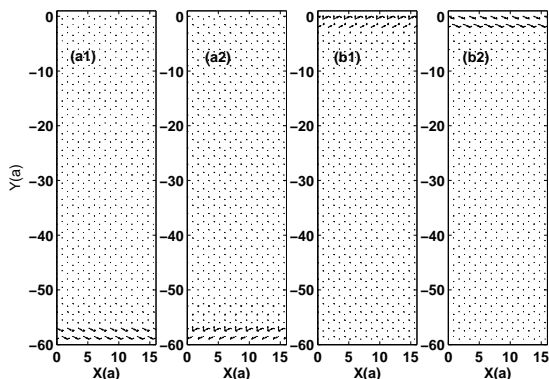


FIG. 3. The local spin-up (a1 and b1) and spin-down (a2 and b2) currents density vector distribution for $\varepsilon_i = 0.1t$, $\lambda_{R1} = 1.0t$ and $\lambda_{R2} = 0.2t$ (QSHE1) with (a) $E = 0.1t$ and (b) $E = -0.1t$.

Next, for QSHE1, the Fermi energy is tuned to $E = 0.1t$ or $E = -0.1t$, reaching slightly into the bulk band. The configurations of spin-dependent local-current-flow

vector in such regions are plotted in Fig. 3. We find that the edge states are not fully spin-filtered when they are inside the bulk band. However, in this case, the electrons flow along the lower edge (see Fig. 3 (a)), while the holes flow forward along the upper edge (see Fig. 3 (b)).

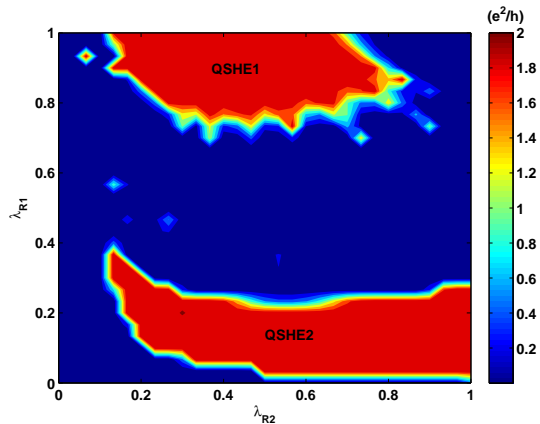


FIG. 4. (color online) Phase diagram showing the conductance G as a function of λ_{R1} and λ_{R2} for fixing $\varepsilon_i = 0.1t$ and $E = 0$.

In order to have a global view on the phase transitions, the phase diagram at $\varepsilon_i = 0.1t$ is plotted in Fig. 4. When these two kinds of spin-orbit couplings are tuned properly, two kinds of QSHE, QSHE1 and QSHE2 appear. For QSHE1, the silicene nanoribbon has a large bulk gap and there are only gapless edge states in the bulk gap because the first spin-orbit coupling can widen the bulk gap.²¹ On the other hand, for QSHE2, the system has a narrow bulk gap and even the gapless edge states is located in the bulk band because the second spin-orbit coupling can narrow the bulk gap.³⁰

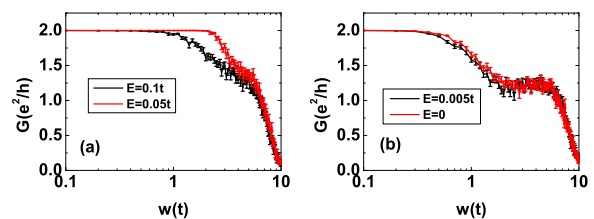


FIG. 5. (color online) The conductance G as a function of the disorder strengths w for (a) $\varepsilon_i = 0.1t$, $\lambda_{R1} = 1.0t$ and $\lambda_{R2} = 0.2t$ (QSHE1) and (b) $\varepsilon_i = 0.1t$, $\lambda_{R1} = 0.05t$ and $\lambda_{R2} = 0.6t$ (QSHE2) with the various energy E . The error bars show standard deviation of the conductance for 100 samples.

Finally, we examine the non-magnetic disorder effect on the conductance plateau $2e^2/h$ of the QSHE. Random on-site potential w_i is added for each site i in the central region, where w_i is uniformly distributed in the range $[-w/2, w/2]$ with the disorder strength w . Figs. 5 (a) and (b) show the conductance G versus the disorder

strength at various energy for QSHE1 and QSHE2, respectively. The results show that these quantum plateaus are robust against non-magnetic disorder because of the topological origin of the edge states. Especially, the quantum plateau of QSHE1 maintains its quantized value very well even when w reaches $2.0t$ for $E = 0.05t$, as shown in Fig. 5 (a). We can also find that the gapless edge states of QSHE1 are more insensitive to the non-magnetic disorder than those of QSHE2 because the bulk gap of QSHE1 is larger than that of QSHE2. With further increasing of the disorder strength, the conductance gradually reduce to zero and the system eventually enters the insulating regime.

In summary, we predict that the QSHE can be induced by applying an electric field in silicene even if the intrinsic spin-orbit coupling is very weak. The energy bands, the configurations of the spin-dependent local-current-flow vector, and the conductance of the system are numerically studied using the tight-binding Hamiltonian. The first and second Rashba spin-orbit couplings, referring to the nearest and next-nearest neighbor hoppings respectively, can be tuned by the external electric field due to the buckled structure of silicene. The staggered sublattice potential induced by the external electric field open a bulk gap and the gapless edge states are built in the gap by the two kinds of Rashba spin-orbit couplings. With the help of spin-dependent local-current-vector configurations, we find that the gapless edge states are indeed spin-filtered. We also find that when the two kinds of Rashba spin-orbit couplings are tuned properly, there are two types of QSHE, QSHE1 with a wide bulk gap and QSHE2 with a narrow bulk gap. Moreover, the gapless edge states have also been found to be robust against non-magnetic disorder.

This work was supported by National Natural Science Foundation of China (Grant Nos. 11104059, 61176089 and 11204294), Hebei province Natural Science Foundation of China (Grant No. A2011208010), and Postdoctoral Science Foundation of China (Grant No. 2012M510523).

¹C. L. Kane and E. J. Mele, Phys. Rev. Lett. **95**, 146802 (2005).

²B. A. Bernevig, T. L. Hughes, and S. C. Zhang, Science **314**, 1757 (2006).

- ³M. König, S. Wiedmann, C. Brüne, A. Roth, H. Buhmann, L. W. Molenkamp, X. L. Qi, and S. C. Zhang, Science **318**, 766 (2007).
- ⁴C. X. Liu, T. L. Hughes, X. L. Qi, K. Wang, and S. C. Zhang, Phys. Rev. Lett. **100**, 236601 (2008).
- ⁵C.-C. Liu, W. Feng, and Y. Yao, Phys. Rev. Lett. **107**, 076802 (2011).
- ⁶Y. G. Yao, F. Ye, X. L. Qi, S. C. Zhang, and Z. Fang, Phys. Rev. B **75**, 041401(R) (2007).
- ⁷D. Huertas-Hernando, F. Guinea, and A. Brataas, Phys. Rev. B **74**, 155426 (2006).
- ⁸H. Min, J. E. Hill, N. A. Sinitsyn, B. R. Sahu, and L. Kleinman, A. H. MacDonald, Phys. Rev. B **74**, 165310 (2006).
- ⁹B. Lalmi, H. Oughaddou, H. Enriquez, A. Kara, S. Vizzini, B. Ealet, and B. Aufray, Appl. Phys. Lett. **97**, 223109 (2010).
- ¹⁰B. Feng, Z. Ding, S. Meng, Y. Yao, X. He, P. Cheng, L. Chen, and K. Wu, Nano Lett. **12**, 3507 (2012).
- ¹¹L. Chen, C.-C. Liu, B. Feng, X. He, P. Cheng, Z. Ding, S. Meng, Y. Yao, and K. Wu, Phys. Rev. Lett. **109**, 056804 (2012).
- ¹²B. Aufray, A. Kara, S. Vizzini, H. Oughaddou, C. Léandri, B. Ealet, and G. Le Lay, Appl. Phys. Lett. **96**, 183102 (2010).
- ¹³P. De Padova, C. Quaresima, C. Ottaviani, P. M. Sheverdyayeva, P. Moras, C. Carbone, D. Topwal, B. Olivieri, A. Kara, H. Oughaddou, B. Aufray, and G. Le Lay, Appl. Phys. Lett. **96**, 261905 (2010).
- ¹⁴Y. Ding and J. Ni, Appl. Phys. Lett. **95**, 083115 (2009).
- ¹⁵M. Houssa, E. Scalise, K. Sankaran, G. Pourtois, V. V. Afanasev, and A. Stesmans, Appl. Phys. Lett. **98**, 083102 (2011).
- ¹⁶Y. Ding and Y. Wang, Appl. Phys. Lett. **100**, 083102 (2012).
- ¹⁷J. Kang, F. Wu, and J. Li, Appl. Phys. Lett. **100**, 233122 (2012).
- ¹⁸M. Houssa, G. Pourtois, V. V. Afanasev, and A. Stesmans, Appl. Phys. Lett. **97**, 112106 (2010).
- ¹⁹S. Cahangirov, M. Topsakal, E. Akturk, H. Sahin, and S. Ciraci, Phys. Rev. Lett. **102**, 236804 (2009).
- ²⁰C. C. Liu, H. Jiang, Y. G. Yao, Phys. Rev. B **84**, 195430 (2011).
- ²¹M. Ezawa, New J. Phys. **14**, 033003 (2012).
- ²²M. Ezawa, Phys. Rev. Lett. **109**, 055502 (2012).
- ²³X. T. An, Y. Y. Zhang, J. J. Liu, and S. S. Li, New J. Phys. **14**, 083039 (2012).
- ²⁴W. Ren, Z. Qiao, J. Wang, Q.-F. Sun, and H. Guo, Phys. Rev. Lett. **97**, 066603 (2006).
- ²⁵M. P. L. Sancho, J. M. L. Sancho, and J. Rubio, I. Phys. F: Met. Phys. **15**, 851 (1985).
- ²⁶B. K. Nikolić, L. P. Zárbo, and S. Souma, Phys. Rev. B **73**, 075303 (2006).
- ²⁷H. Jiang, L. Wang, Q.-F. Sun, and X. C. Xie, Phys. Rev. B **80**, 165316 (2009).
- ²⁸Y. Xing, L. Zhang, and J. Wang, Phys. Rev. B **84**, 035110 (2011).
- ²⁹A.-P. Jauho, N. S. Wingreen, and Y. Meir, Phys. Rev. B **50**, 5528 (1994).
- ³⁰M. Ezawa, Eur. Phys. J. B **85**, 363 (2012).